Int J Thermophys (2010) 31:227–252
DOI 10.1007/s10765-010-0727-7

Soft Repulsion and the Behavior of Equations of State at High Pressures

Olga L. Boshkova · Ulrich K. Deiters

Received: 7 September 2009 / Accepted: 11 March 2010 / Published online: 30 March 2010

Abstract The so-called characteristic curves of Brown—the Amagat (Joule inversion), Boyle, and Charles (Joule–Thomson inversion) curves—of hydrogen are calculated with several equations of state. This work demonstrates that not all equations can generate physically reasonable Amagat curves. After inclusion of corrections for soft repulsion (based on the Weeks–Chandler–Andersen perturbation theory) and quantum effects into the *simplified perturbed-hard-chain theory* (SPHCT) equation of state, this equation is able to not only generate an Amagat curve, but also predict *pVT* data, residual Gibbs energies, and heat capacities of several gases at and above 100 MPa reasonably well.

Keywords Equation of state · Perturbation theory · Soft repulsion · Joule inversion curve · Amagat curve · Brown's characteristic curves · Hydrogen

List of symbols

A	Helmholtz energy
B	2nd virial coefficient
C_p	Isobaric heat capacity
C_V	Isochoric heat capacity
c	Chain length parameter of the SPHCT EOS
d	Apparent hard-sphere diameter
d_0	d at zero density
H	Enthalpy
h	Planck's constant

O. L. Boshkova · U. K. Deiters (✉)
Institute of Physical Chemistry, University of Cologne, Luxemburger Str. 116, 50939 Köln, Germany
e-mail: ulrich.deiters@uni-koeln.de

k_B Boltzmann's constant
m Molecular mass; chain length parameter of the PC-SAFT EOS
N Number of molecules
n Amount of substance
p Pressure
R Universal gas constant
r Intermolecular distance
T Temperature
U Internal energy
u Pair potential
V Volume
v^* EOS size parameter
y Background correlation function
Z Compressibility factor
α_p Isobaric thermal expansivity
δ Perturbation theory integral, Eq. 20
ϵ Lennard-Jones potential energy parameter
κ_T Isothermal compressibility
Λ Thermal de Broglie wavelength
π_T Internal pressure
ρ Density
σ Lennard-Jones potential size parameter
ξ Reduced density

Subscripts

att Attraction
c Critical
hs Hard sphere
m Molar property

Superscripts

r Residual property
~ Reduced property

1 Introduction

Equations of state for fluids play a major role not only in fundamental thermodynamics, but also in many applied sciences, from chemical engineering to geochemistry. Nowadays there are thousands of equations of state in use, which differ not only quantitatively (i.e., in the deviation with which a given set of experimental data can be correlated), but also qualitatively.

In order to assess these qualitatitve features, Brown [1] proposed the calculation of several characteristic curves for equations of state, among them curves that he called the Amagat, Boyle, and Charles curves. (Their definitions are given in the

following section.) The curves were later used in the IUPAC "Guidelines for publication of equations of state" [2]; their calculation has become a kind of standard test for so-called reference equations of state.

Of these characteristic curves, the Amagat (or Joule inversion) curve is rather difficult to obtain; in fact, it does not exist for most equations of state. Most users of equations of state, however, have never been aware of this shortcoming, for the Amagat curve is located at rather extreme pressures or temperatures (100 to 200 times the critical pressure, 20 times the critical temperature). For most substances, these conditions cannot be reached experimentally, and therefore the Amagat curve is not of practical relevance, but rather "science fiction."

But there are exceptions: for hydrogen, a substance of rapidly increasing technological importance, parts of the Amagat curve are experimentally accessible with standard autoclave technology. For methane and some other components of natural gas, the Amagat curve could be reached in deep reservoirs. Conversely, equations of state that are used to model such reservoirs or applied to compressed hydrogen should be able to produce an Amagat curve.

Here, however, a problem is encountered:

- High-quality reference equations of state of the Bender/Jacobsen-Stewart [3,4] or Wagner–Setzmann [5] type have the quality and flexibility to generate Amagat curves—but determining parameters for new fluids is a time-consuming and demanding task, and they can be used for pure fluids only. A notable exception is the GERG equation [6], an extension of the Bender/Jacobsen-Stewart-type equation toward mixtures by a heroic effort; but its valid pressure range is usually below the Amagat curve region.
- On the other hand, semiempirical or theoretical equations of state can be applied to mixtures—but they usually fail to produce Amagat curves because they contain hard-core repulsion terms, whereas the Amagat curve is related to soft repulsion.

Of course there have been many attempts over the previous decades to account for soft repulsion in equations of state using temperature-dependent molecular size parameters, but this approach can lead to unphysical behavior, as pointed out already by Trebble et al. [7,8]. In this work, we compare the behavior of several equations of state. We demonstrate how a theory-based equation of state can be equipped with soft-repulsion features, and thus can be made fit for thermodynamic studies under extreme conditions.

2 Theory

2.1 The Characteristic Curves

The characteristic curves proposed by Brown [1], sometimes referred to as "ideal" curves, are loci where a fluid shows some of the features of an ideal gas. As a example, Fig. 1 shows the first-order characteristic curves of hydrogen, computed from the equation of state of Leachman et al. [9], along which some first-order derivatives of the compressibility factor have "ideal values."

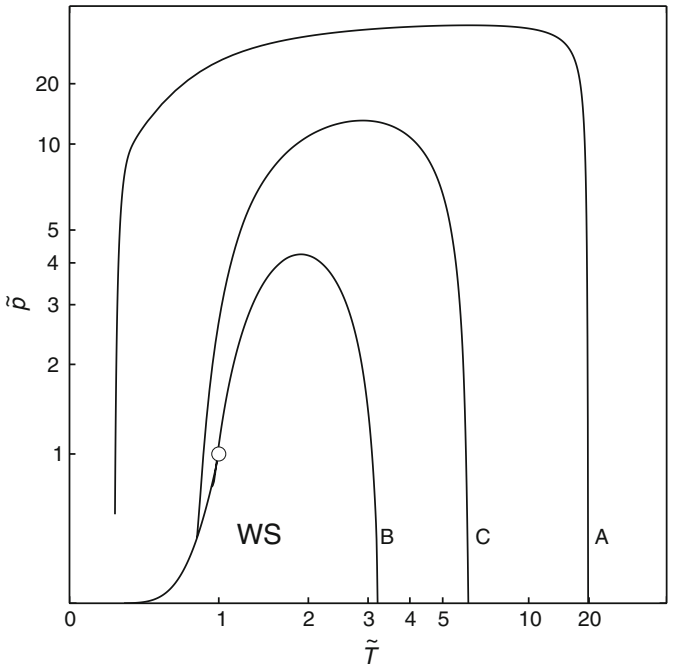

Fig. 1 Characteristic curves of hydrogen, computed with the empirical equation of state of Leachman et al. [9]. *A* Amagat (Joule inversion) curve, *B* Boyle curve, *C* Charles (Joule–Thomson inversion) curve, *open circle* critical point. The coordinates have been distorted with the function $x \rightarrow x/(1 + 3x_c)$ with $x = T$, p for better visibility of details

2.1.1 The Boyle Curve

This curve is defined by any one of the following mathematical criteria (p pressure, V volume, T temperature, $Z = pV/(nRT)$ compressibility factor, n amount of substance):

$$\left(\frac{\partial Z}{\partial V}\right)_T = 0 \qquad \left(\frac{\partial Z}{\partial p}\right)_T = 0 \qquad \left(\frac{\partial p}{\partial V}\right)_T = -\frac{p}{V} \tag{1}$$

Along the Boyle curve, the compressibility factor does not depend on volume or pressure during isothermal changes. This curve exists for practically all equations of state. It starts at zero pressure at the Boyle temperature (the temperature at which the 2nd virial coefficient goes to zero), passes over a maximum, and ends near (but not at) the critical point on the saturation curve (more accurately, on the spinodal).

2.1.2 The Charles Curve

The Charles curve or Joule–Thomson inversion curve is the locus along which the isenthalpic expansion coefficient vanishes. The mathematical criterion is any one of these (H enthalpy):

$$\left(\frac{\partial Z}{\partial T}\right)_p = 0 \quad \left(\frac{\partial Z}{\partial V}\right)_p = 0 \quad \left(\frac{\partial T}{\partial p}\right)_H = 0 \quad \left(\frac{\partial H}{\partial p}\right)_T = 0 \quad \left(\frac{\partial V}{\partial T}\right)_p = \frac{V}{T} \tag{2}$$

This curve originates at a point on the T axis where the slope of the 2nd virial coefficient function, $B(T)$, matches that of a secant from the origin:

$$\frac{\mathrm{d}B}{\mathrm{d}T} = \frac{B}{T} \tag{3}$$

It passes over a maximum and ends on the saturation curve at a lower temperature than the Boyle curve. The Charles curve is always outside the Boyle curve.

2.1.3 The Amagat Curve

It is also known as the Joule inversion curve. Along this curve, the internal pressure changes its sign. This happens because high pressure or high temperature (collisions at high speed) forces the molecules into the repulsive regions of their pair potentials. The mathematical criterion is any one of the following (U internal energy):

$$\left(\frac{\partial Z}{\partial T}\right)_V = 0 \quad \left(\frac{\partial Z}{\partial p}\right)_V = 0 \quad \left(\frac{\partial U}{\partial V}\right)_T = 0 \quad \left(\frac{\partial p}{\partial T}\right)_V = \frac{p}{T} \tag{4}$$

This curve owes its existence to softly repulsive pair potentials; this is discussed in Sect. 2.2. It starts on the T axis at the (usually very high) temperature where the 2nd virial coefficient has a maximum ($\mathrm{d}B/\mathrm{d}T = 0$) and runs to lower temperatures, passing through a maximum. It encloses the Boyle and the Charles curves. If an equation of state cannot generate a maximum of the 2nd virial coefficient, its Amagat curve does not exist.

2.2 Thermodynamic Considerations

Many equations of state, especially those with a theoretical foundation, are of the van der Waals type, i.e., they consist of a repulsion and an attraction term. Here, we are considering a special, although very common, equation type having the general structure

$$p = \frac{RT}{V_\mathrm{m}} Z_\mathrm{hs}(\xi) - p_\mathrm{att}(\xi, \tilde{T}). \tag{5}$$

The repulsion term contains the compressibility factor of the hard-sphere (or another hard-core) fluid, which depends on the reduced density $\xi = v^*/V_\mathrm{m}$ *only*; v^* denotes a characteristic volume. The attraction term p_att usually depends on the reduced density and the reduced temperature $\tilde{T} = T/T^*$, with T^* denoting a characteristic temperature. For properly designed equations of state, however, the temperature dependence decreases with increasing temperature. It is therefore permissible to neglect the

attraction term in calculations of properties that depend on temperature derivatives at high temperatures.

Real molecules are no hard-core particles, but allow some interpenetration of their repulsive cores. This "soft repulsion" is accounted for in equations of state of the type (5) by letting the dimensions of the hard cores become temperature-dependent. It should be noted that, as long as chemical reactions or deformations of molecules are ruled out, soft repulsion is the only mechanism that can bring about a positive configurational energy in classical fluids[1]; the contribution of the attractive potential well is always negative. Therefore, a change of the sign of the internal pressure,

$$\pi_T = \left(\frac{\partial U}{\partial V}\right)_T, \tag{6}$$

and thus the existence of the Amagat curve, is related to soft repulsion.

An accurate study of the high-temperature/high-pressure limiting behavior of *cubic* equations of state was published by Trebble and Bishnoi [7] and by Salim and Trebble [8]. In this special case, the repulsion term is

$$Z_{\mathrm{hs}} = \frac{V_{\mathrm{m}}}{V_{\mathrm{m}} - v^*}, \tag{7}$$

and its contributions to the internal energy and the residual isochoric heat capacity are

$$U^{\mathrm{r}}_{\mathrm{m}}(V_{\mathrm{m}}, T) = -pTv^{*\prime} \quad \text{with} \quad v^{*\prime} = \frac{\mathrm{d}v^*}{\mathrm{d}T} \tag{8}$$

and

$$C^{\mathrm{r}}_{V,\mathrm{m}}(V_{\mathrm{m}}, T) = -p\left[2v^{*\prime} + Tv^{*\prime\prime} + \frac{p(v^{*\prime})^2}{R}\right]. \tag{9}$$

As the curvature of $v^*(T)$ must be positive at least at high temperatures, and as the second and third term will overrule the first one at high temperatures or pressures, $C^{\mathrm{r}}_{V,\mathrm{m}}$ will necessarily turn negative under such conditions.

While negative *total* isochoric heat capacities are of course in conflict with the thermodynamic stability rules, this is not necessarily the case for *residual* heat capacities. Still, negative $C^{\mathrm{r}}_{V,\mathrm{m}}$ should usually not occur in reality: as a fluid is compressed from a low-density, ideal-gas state to liquid-like densities, the interaction with neighbor molecules lets translational degrees of freedom become vibrational ones, and rotational degrees of freedom librational ones. Each vibrational and librational degree of freedom, however, contributes up to R to the molar isochoric heat capacity, whereas translational and rotational degrees contribute $R/2$ only. Therefore, real fluids should

[1] Quantum fluids are discussed in Sect. 2.4.

have higher isochoric heat capacities, and $C^{\mathrm{r}}_{V,\mathrm{m}}$ should be positive. Negative $C^{\mathrm{r}}_{V,\mathrm{m}}$ values are usually artifacts.[2]

Consequently, Salim and Trebble recommended keeping the size parameter temperature-independent. This avoids the prediction of unphysical values, but either makes equations of state inaccurate at high temperatures or pressures, or it tempts the developers of equations of state to compensate for this deficiency by creating a very complicated attraction term, which usually leads to further problems.

Incidentally, the internal pressure of cubic equations of state (disregarding the attraction term) is

$$\pi_T = \frac{p^2 v^{*\prime}}{R}. \tag{10}$$

Unless $v^*(T)$ has an extremum or the attraction term has a very unusual temperature dependence at high temperatures (so that it cannot be neglected at high temperatures), the internal pressure cannot change sign, and hence the Amagat curve cannot exist for cubic equations of state.

The dilemma can eventually be avoided using noncubic equations of state. In this more general case, the residual internal energy (without attraction contributions) is

$$U^{\mathrm{r}}_{\mathrm{m}}(V_{\mathrm{m}}, T) = -RT^2(Z_{\mathrm{hs}} - 1)\frac{v^{*\prime}}{v^*} \tag{11}$$

and for the isochoric heat capacity

$$C^{\mathrm{r}}_{V,\mathrm{m}}(V_{\mathrm{m}}, T) = -\frac{RT}{v^*}(Z-1)\left[2v^{*\prime} + Tv^{*\prime\prime} - T\frac{(v^{*\prime})^2}{v^*}\right] - V_{\mathrm{m}}\frac{v^{*\prime}}{v^*}(p'T - p). \tag{12}$$

At high pressures and temperatures there must be a positive contribution to the internal energy. When $Z - 1$ is positive, Eq. 11 implies $v^{*\prime} < 0$, i.e., the apparent hard-body size decreases with temperature.

In Eq. 12, the first and the third terms give positive contributions to the heat capacity. The second term contains the curvature of v^* with respect to temperature, which should be positive at least at high temperatures; consequently this term can give a large *negative* contribution. The last term of Eq. 12 contains the expression $(p'T - p)$, which is the internal pressure, $(\partial U/\partial V)_T$. This property is positive inside the Amagat curve and negative outside; at very high temperatures, it gives a positive contribution to $C^{\mathrm{r}}_{V,\mathrm{m}}$. It is therefore no longer possible to make a general prediction about the limiting behavior of the residual isochoric heat capacity: properly designed noncubic equations of state can have positive $C^{\mathrm{r}}_{V,\mathrm{m}}$ values at high temperatures.

[2] An exception can be caused by quantum effects, which decrease the number of accessible energy levels with increasing density. This will be discussed in Sect. 2.4.

For the sake of completeness we briefly consider the behavior of residual isobaric heat capacities: the difference of isobaric and isochoric heat capacities is given by the well-known relation,

$$C_{p,\mathrm{m}} - C_{V,\mathrm{m}} = \frac{\alpha_p^2 V T_\mathrm{m}}{\kappa_T}, \tag{13}$$

where α_p is the isobaric thermal expansivity and κ_T the isothermal compressibility. For an ideal gas this difference amounts to R. Hence, the residual isobaric heat capacity can be written as

$$C^\mathrm{r}_{p,\mathrm{m}} = C^\mathrm{r}_{V,\mathrm{m}} + \frac{\alpha_p^2 V T_\mathrm{m}}{\kappa_T} - R. \tag{14}$$

Because of the $-R$ term, $C^\mathrm{r}_{p,\mathrm{m}}$ can possibly become negative even if $C^\mathrm{r}_{V,\mathrm{m}} > 0$. For most fluids under most conditions the second term on the right-hand side of Eq. 14 outweighs the $-R$. But liquid water near its freezing temperature is a known exception.

2.3 Perturbation Theory

A powerful method for dealing with soft repulsions between molecules was proposed by Weeks, Chandler, and Andersen more than three decades ago [10]. We summarize the approach for the reader's convenience.

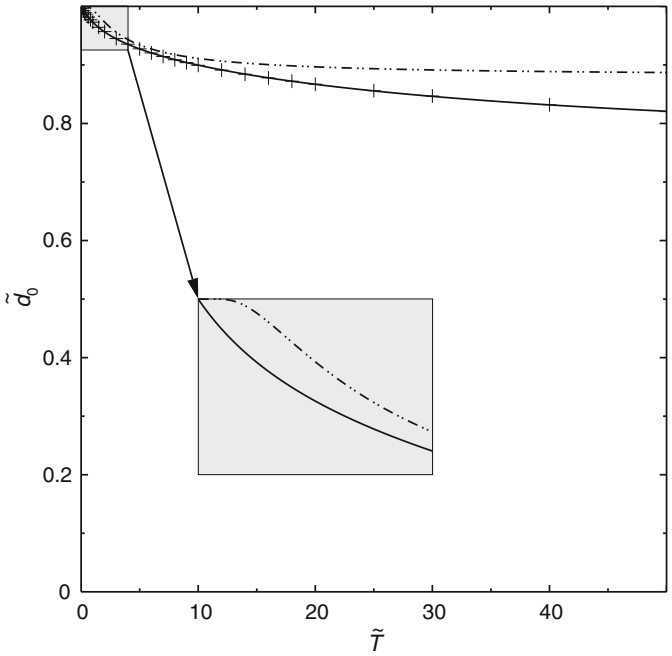

Fig. 2 Apparent reduced hard-sphere diameter for a truncated Lennard-Jones potential as a function of reduced temperature. + Eq. 19; — interpolation function, Eq. 22; – ··· – PC-SAFT, Eq. 28 [19,20]

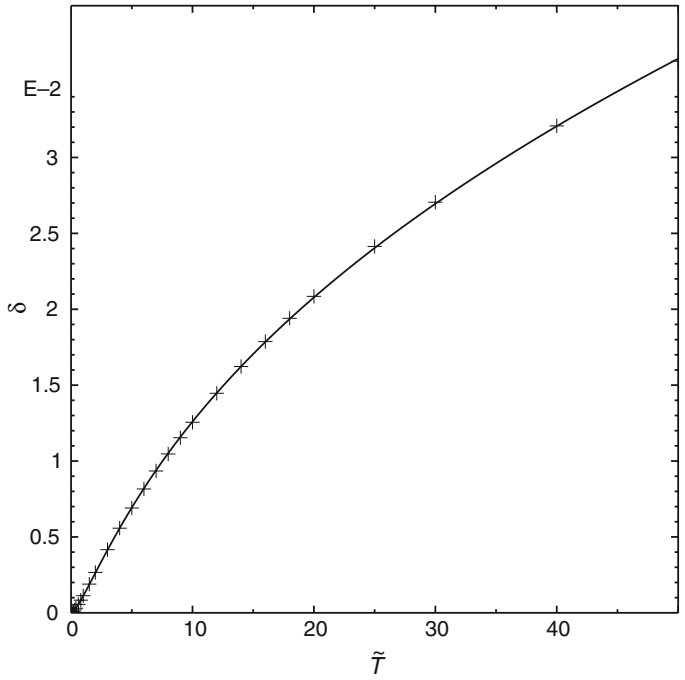

Fig. 3 δ integral for a truncated Lennard-Jones potential as a function of reduced temperature. + evaluation of the integral, Eq. 20; — interpolation function, Eq. 23

Consider a steep, softly repulsive pair potential, e.g., a truncated Lennard-Jones 12-6 potential:

$$u(r) = \begin{cases} r \le \sigma\colon 4\epsilon \left(\left(\frac{\sigma}{r}\right)^{12} - \left(\frac{\sigma}{r}\right)^{6} \right) \\ r > \sigma\colon 0 \end{cases} \tag{15}$$

Here, ϵ denotes the potential well depth, and σ the zero distance of the potential. As we merely want to introduce a softness correction into an existing equation of state, the truncation of the Lennard-Jones potential at $r = \sigma$ is preferable over one at the minimum, $r = 2^{1/6}\sigma$. It can then be shown that the Helmholtz energy of a fluid with this interaction potential is—to a good approximation—the same as that of a hard-sphere fluid with a collision diameter determined in such a way that the integral of the so-called blip function vanishes:

$$\int_0^\infty \left(\exp\left(-\frac{u(r)}{k_\mathrm{B}T}\right) - \exp\left(-\frac{u_\mathrm{hs}(r)}{k_\mathrm{B}T}\right) \right) y_\mathrm{hs}(r,\xi) r^2 \,\mathrm{d}r = 0 \quad \text{with} \quad \xi = \frac{\pi}{6} N d^3 \tag{16}$$

Here, ξ is the reduced density with respect to the hard-sphere diameter d. $y_{\mathrm{hs}}(r,\xi)$ denotes the background correlation function of a hard-sphere fluid. The second exponential term represents a Heaviside step function (i.e., a single unit step) located at the distance d.

Verlet and Weis proposed a method for solving this equation for d [11,12]. As the integrand of Eq. 16 differs from zero over a rather narrow range only, it is sufficient to approximate $y_{\mathrm{hs}}(r)$ by the first two terms of its Taylor expansion around d:

$$y_{\mathrm{hs}}(\tilde{r},\xi) = y_0(\xi) + y_1(\xi)(\tilde{r}-1) + \cdots \quad \text{with} \quad \tilde{r} = \frac{r}{d} \tag{17}$$

With this approximation the following expression for the hard-sphere diameter can be obtained from Eq. 16,

$$d = \frac{d_0}{1 - \frac{y_1(\xi)\delta}{2y_0(\xi)}}, \tag{18}$$

where d_0 is an effective hard-sphere diameter at zero density,

$$\tilde{d}_0 = \frac{d_0}{\sigma} = \int_0^\infty \left(\exp\left(-\frac{\tilde{u}(\tilde{r})}{\tilde{T}} \right) - 1 \right) \mathrm{d}\tilde{r} \tag{19}$$

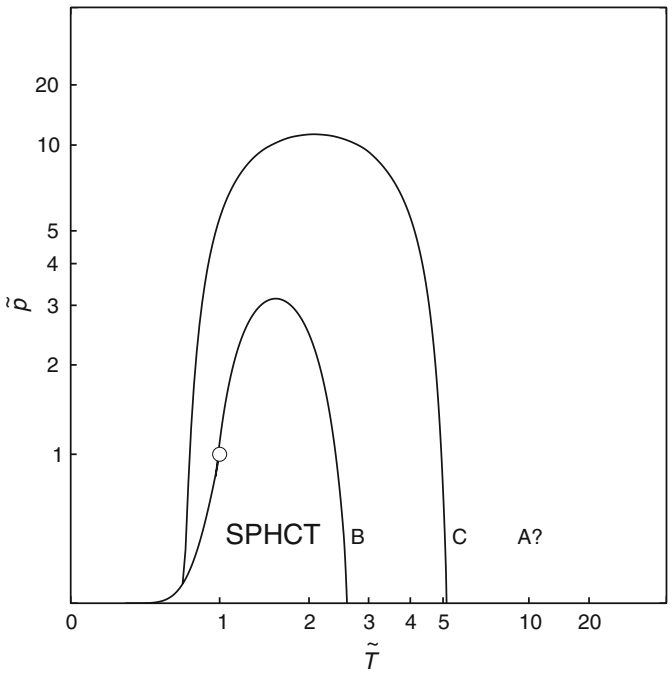

Fig. 4 Characteristic curves of hydrogen, computed with the SPHCT equation of state [15]. For an explanation of the symbols see Fig. 1. There is no Amagat curve for this equation

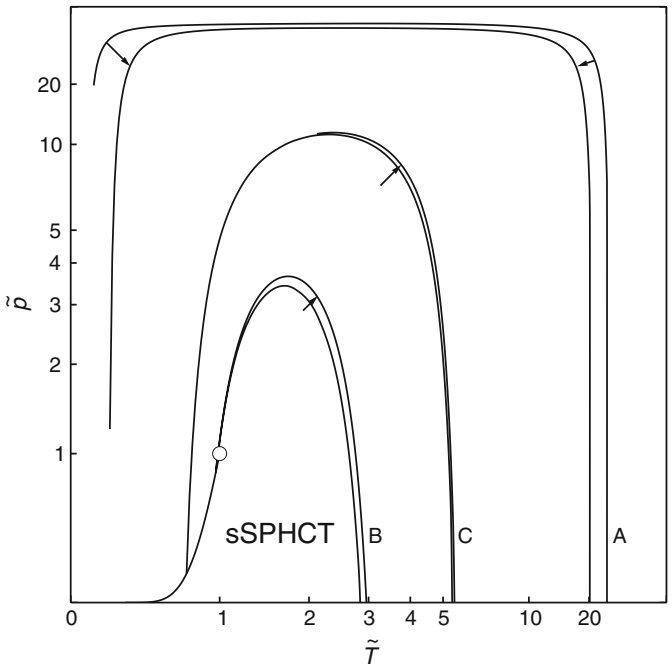

Fig. 5 Characteristic curves of hydrogen, computed with the soft-core SPHCT equation of state (this work). For an explanation of the symbols, see Fig. 1. The *arrows* indicate the effect of the quantum correction

with

$$\tilde{u}(\tilde{r}) = \frac{1}{\epsilon} u\left(\frac{r}{\sigma}\right), \quad \tilde{T} = \frac{k_B T}{\epsilon}$$

and δ a perturbation integral of higher order:

$$\delta = \int_0^\infty (\tilde{r} - 1)^2 \frac{\mathrm{d}}{\mathrm{d}\tilde{r}} \exp\left(-\frac{\tilde{u}(\tilde{r})}{\tilde{T}}\right) \mathrm{d}\tilde{r} \tag{20}$$

$y_0(\xi)$ and $y_1(\xi)$ in Eq. 19 are properties of the hard-sphere reference fluid only. Verlet and Weis proposed a universal approximation function:

$$\frac{y_1(\xi)}{2y_0(\xi)} = \frac{1 - 4.25\xi' + 1.362\xi'^2 - 0.8751\xi'^3}{(1 - \xi')^2} \quad \text{with} \quad \xi' = \xi - \frac{1}{16}\xi^2 \tag{21}$$

$\tilde{d}_0$ and δ depend on temperature only; for the truncated Lennard-Jones potential Eq. 15, the integrals Eqs. 19 and 20 were evaluated numerically and approximated by (see Figs. 2, 3)

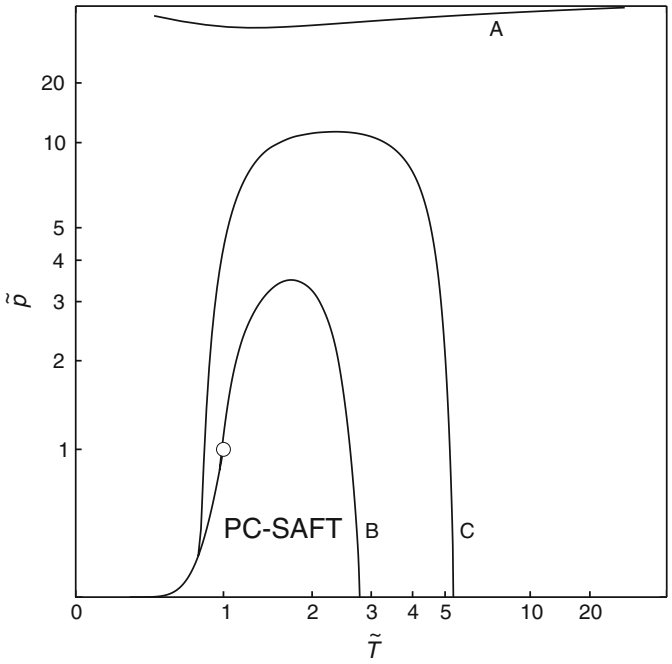

Fig. 6 Characteristic curves of hydrogen, computed with the PC-SAFT equation of state [19,20]. For an explanation of the symbols, see Fig. 1

$$\tilde{d}_0 = \frac{1 + f_{11}\tilde{T} + f_{12}\tilde{T}^2}{1 + f_{21}\tilde{T} + f_{22}\tilde{T}^2} \tag{22}$$

and

$$\delta = \frac{g\tilde{T}^{3/2}}{1 + \frac{1}{4}\tilde{T}} \tag{23}$$

with $f_{11} = 0.437\,814\,2$, $f_{12} = 0.009\,951\,898$, $f_{21} = 0.474\,555\,8$ and $f_{22} = 0.013\,387\,17$, and $g = 0.001\,394\,056$. As ξ and ξ' depend on d, it is necessary to solve Eq. 18 iteratively. This is a complication, but even a simple successive substitution scheme converges well [12]; we propose to use Steffensen's accelerated substitution method, which guarantees 2nd-order convergence [13].

If the iteration is turned off, i.e., if a temperature-dependent, but density-independent hard-sphere diameter $d = d_0$ is used, the WCA perturbation theory reduces to the so-called Barker–Henderson (BH) approximation.

2.4 Equation of State

It should be emphasized that the Weeks–Chandler–Andersen perturbation theory leads to a temperature- and density-dependent effective hard-sphere diameter.

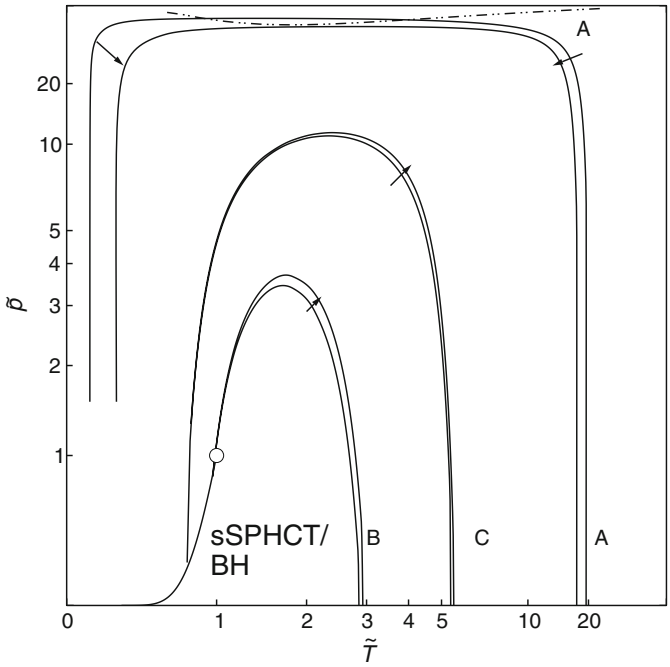

Fig. 7 Characteristic curves of hydrogen, computed with the soft-core SPHCT equation of state with density-independent size parameter, temperature dependence taken from: — Barker–Henderson perturbation theory, – ··· – PC-SAFT equation of state. For an explanation of the other symbols, see Fig. 1

Several authors realized that using this diameter with a hard-sphere equation would lead to equations of state for realistic fluids of high quality, but they regarded this approach as not feasible, or at least inconvenient [14], because the calculation of the hard-sphere diameter requires an iteration.

It turns out however that the iteration with Steffensen's method is reliable and very fast. Alternatively, one could represent $\tilde{d}(\xi, \tilde{T})$ by a suitable 2-dimensional interpolation function. But the evaluation of such a function would introduce inaccuracies and probably not save much time over the iteration.

For the demonstration of the effect of the softness correction we use the *simplified perturbed-hard-chain theory* (SPHCT) equation of state [15]. It contains a hard-sphere term with a modification to account for chain molecules and an attractive term based on an approximate theory of the square-well fluid. The expression for the residual Helmholtz energy is

$$\frac{A_{\mathrm{m}}^{\mathrm{r}}}{RT} = \frac{c(4\xi - 3\xi^2)}{(1-\xi)^2} - zc \ln\left(1 + \frac{6}{\pi\sqrt{2}}\,\xi\left(\exp\left(\frac{1}{2\tilde{T}}\right) - 1\right)\right) \quad \text{with} \quad \tilde{\xi} = \frac{v^*}{V} = \frac{\pi}{6}\frac{N\sigma^3}{V}. \tag{24}$$

Here, c is a parameter accounting for nonspherical shape (density-dependent degrees of freedom); $z = 18$ is a coordination number.

The "soft-core SPHCT" equation of state (sSPHCT) is obtained from Eq. 24 simply by replacing σ in the repulsion term with the perturbation theory diameter d from Eq. 18. As this is a function of temperature and density, it is no longer possible to give an explicit expression for the pressure. Instead, we use numerical differentiation. The formula

$$Z = 1 + \frac{\rho}{RT}\left(\frac{A_{\mathrm{m}}^{\mathrm{r}}(\rho + \Delta\rho, T) - A_{\mathrm{m}}^{\mathrm{r}}(\rho - \Delta\rho, T)}{2\Delta\rho} + O(\Delta\rho^2)\right) \tag{25}$$

with $\Delta\rho \approx 10^{-5}\rho$ and $\rho = n/V$ (using "double precision" arithmetic) was found to be adequate for most purposes [16]. For the implementation in the *ThermoC* program package [17], a 4-point formula was used, which is even good to order $O(\Delta\rho^4)$.

For calculation of thermodynamic properties of hydrogen, it is advisable to include quantum corrections. Here, we use the 1st-order term of the perturbation expansion with respect to Planck's constant h for the hard-sphere fluid [18]:

$$\frac{\Delta A_{\mathrm{m,qc}}}{RT} = 3\sqrt{2}\frac{\Lambda}{d}\frac{\xi - \frac{\xi^2}{2}}{(1-\xi)^3} \quad \text{with} \quad \Lambda = \frac{h}{\sqrt{2\pi m k_{\mathrm{B}} T}} \tag{26}$$

Λ is the thermal de Broglie wavelength, and m is the molecular mass. The softness correction is applied to d and ξ.

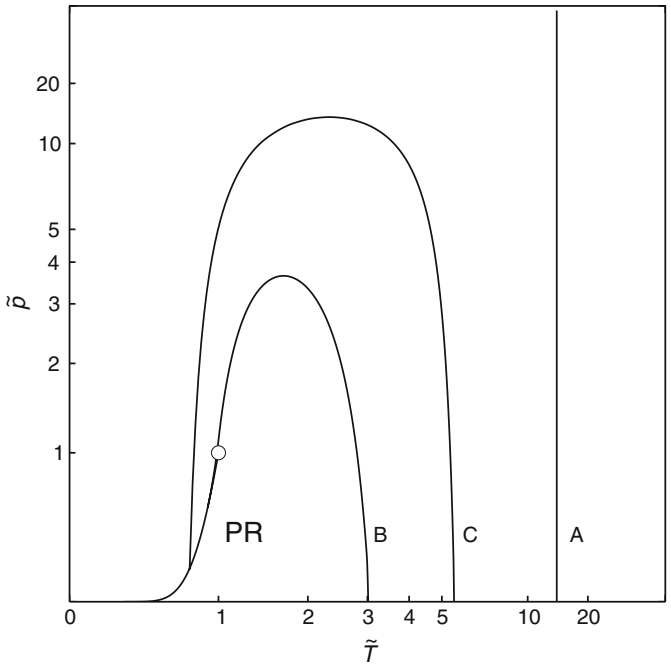

Fig. 8 Characteristic curves of hydrogen, computed with the Peng–Robinson equation of state [21]. For an explanation of the symbols, see Fig. 1

It should be noted that this quantum correction gives a positive contribution to the internal energy,

$$\frac{\Delta U_{\mathrm{m,qc}}}{RT} = -T\frac{\partial(A_{\mathrm{m,qc}}/RT)}{\partial T}, \tag{27}$$

which decreases with increasing temperature. Consequently, there is a negative contribution to the residual isochoric heat capacity.

3 Results and Discussion

3.1 Characteristic Curves

The characteristic curves, discussed in Sect. 2.1 should all exist, have a single maximum and no inflection points. As mentioned before, the Amagat curve must enclose the Charles curve, and this must enclose the Boyle curve.

The substance-specific parameters of all equations of state used here were calculated from the critical pressure and temperature.

The empirical equation of Leachman et al. [9] represents an actual summary of all available, critically assessed experimental data. Although these data do not extend

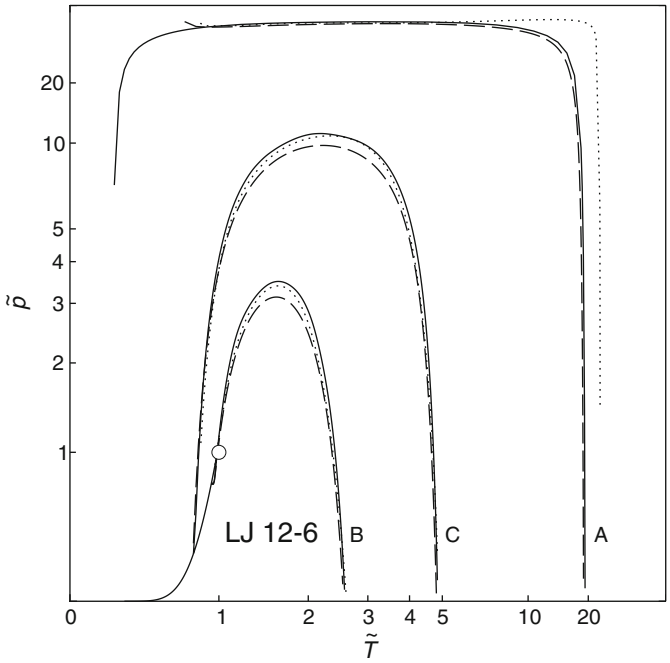

Fig. 9 Characteristic curves of hydrogen, computed with three equation of state for the Lennard-Jones fluid: · · · · · · Johnson et al. [23], - - - Kolafa and Nezbeda [14], — Mecke et al. [24]. For an explanation of the symbols, see Fig. 1

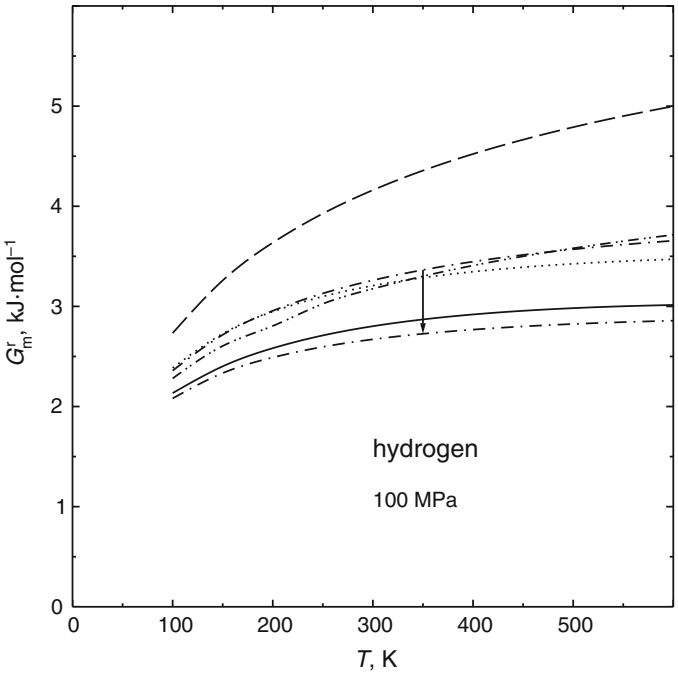

Fig. 10 Prediction of the residual molar Gibbs energy of hydrogen at 100 MPa with several equations of state. — Leachman et al. [9], - - - SPHCT [15], –·– sSPHCT (this work), WCA perturbation theory, ····· sSPHCT, BH perturbation theory, –··– sSPHCT, PC-SAFT temperature dependence. The *arrow* indicates the effect of the quantum corrections

into the Amagat region, the extrapolation qualities of this equation appear to be good enough to calculate a realistic-looking Amagat curve (see Fig. 1).

The original SPHCT equation of state [15] contains a hard-core repulsion term and therefore cannot produce an Amagat curve (see Fig. 4).

After inclusion of the soft-core correction, however, the Amagat curve can be calculated (see Fig. 5), and is remarkably close to the result of the empirical equation of Leachman et al. The predicted maximum of the Amagat curve is at 135 MPa, whereas the empirical equation gives 105 MPa to 116 MPa. For a prediction without any additional adjustable parameters, this is quite good. The deviations of the Amagat curves at low temperatures may be due to insufficient corrections for quantum effects; the convergence of the perturbation expansion of which Eq. 26 is the first term is uncertain at high densities.

The more modern PC-SAFT equation [19,20] contains a hard-chain repulsion term with a semiempirical temperature-dependent core diameter, but no density dependence of the softness correction. The prediction of the Amagat curve gives unphysical results (see Fig. 6). It must be noted of course that this equation was designed primarily for chain molecules under technical conditions, but not for the extreme application considered in this work.

$$\frac{A^{\mathrm{r}}_{\mathrm{m}}}{RT} = m\frac{4\xi - 3\xi^2}{(1-\xi)^2} - (m-1)\ln g^+ - \frac{6\xi_0}{\tilde{T}}\left(2I_1 + m\frac{I_0}{h\tilde{T}}\right) \tag{28}$$

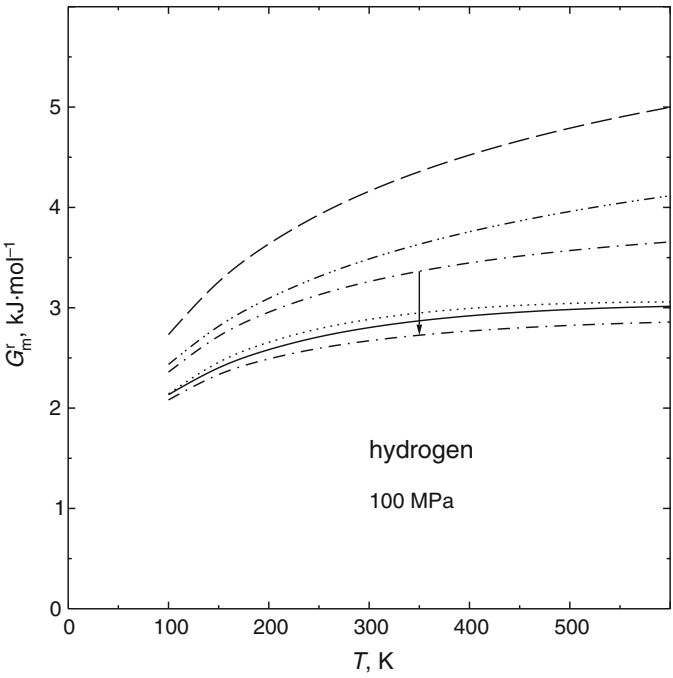

Fig. 11 Prediction of the residual molar Gibbs energy of hydrogen at 100 MPa with several equations of state. — Leachman et al. [9], - - - SPHCT [15], –·– sSPHCT (this work), –··– PC-SAFT [19,20], ····· Peng–Robinson [21]. The *arrow* indicates the effect of the quantum corrections

with

$$\xi_0 = \frac{m v^*}{V_m}$$
$$\xi = \xi_0 \left(1 - 0.12 \mathrm{e}^{-3/\tilde{T}}\right)$$
$$g^+ = \frac{1 - \frac{\xi}{2}}{(1-\xi)^3}$$
$$h = 1 + m\frac{8\xi - 2\xi^2}{(1-\xi)^4} + (1-m)\frac{20\xi - 27\xi^2 + 12\xi^3 - 2\xi^4}{(1-\xi)^2(2-\xi)^2}$$

Here, m denotes the number of chain segments, v^* their molar volume, and g^+ the contact value of the radial distribution function of the hard-sphere fluid; the I_i are polynomials of the reduced density with fixed coefficients.

The failure of the PC-SAFT equation to produce an acceptable Amagat curve may be due to two reasons, namely,

(a) using a density-independent size parameter
(b) or a less than optimal choice of its temperature dependence.

It must be noted that the temperature dependence of the hard-sphere diameter of the PC-SAFT equation differs somewhat from the perturbation theory result, Eq. 19.

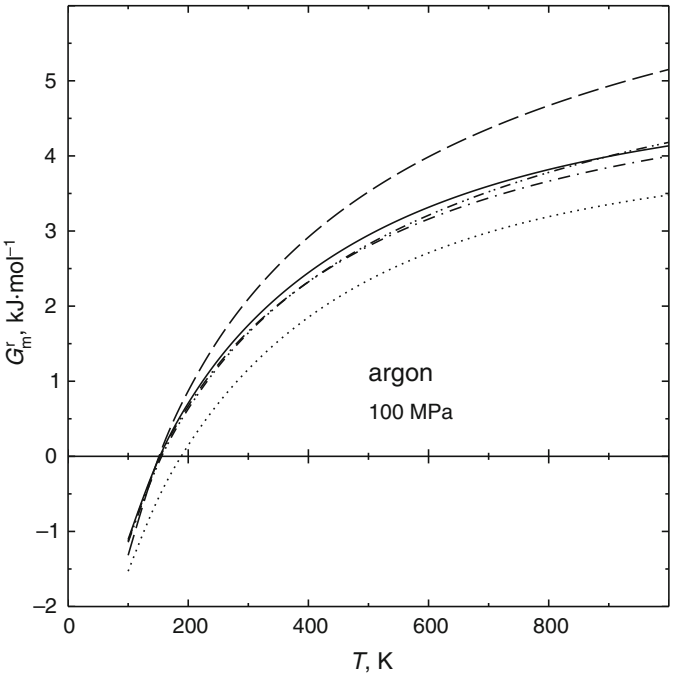

Fig. 12 Prediction of the residual molar Gibbs energy of argon at 100 MPa with several equations of state. — Tegeler et al. [25]; for an explanation of the other symbols, see Fig. 11

The deviations are not very large, as Fig. 2 shows, but there is an important qualitative difference: the temperature function of the PC-SAFT equation is based on a Boltzmann factor and thus contains an inflection point.

In order to identify the reason for the problems of the PC-SAFT equation, we computed the characteristic curves of an sSPHCT equation with the temperature dependence of the size parameter either given by Eq. 22 (i.e., density-independent, equivalent to Barker–Henderson perturbation theory) or by the PC-SAFT size parameter function. The results are shown in Fig. 7, with the temperature dependence obtained from BH perturbation theory, the SPHCT equation generates a meaningful Amagat curve; the effect of the density dependence introduced by the WCA theory is rather small. With the PC-SAFT temperature dependence, a physically unreasonable Amagat curve is obtained. It seems therefore that cause (b) is responsible for the failure of the PC-SAFT equation, and that temperature dependencies based on simple Boltzmann functions should be avoided.

The Peng–Robinson equation [21] is representative of the class of cubic equations of state. It uses a temperature-dependent attraction parameter for improved representation of the saturation curve; the temperature function $\alpha(T)$ was proposed by Soave [22] and contains Pitzer's acentric factor ω as an additional parameter.

$$\frac{A^{\mathrm{r}}_{\mathrm{m}}}{RT} = -\ln(1-\xi) - \frac{a}{2\sqrt{2}RTv^*}\ln\left(\frac{1+(\sqrt{2}+1)\xi}{1-(\sqrt{2}-1)\xi}\right) \tag{29}$$

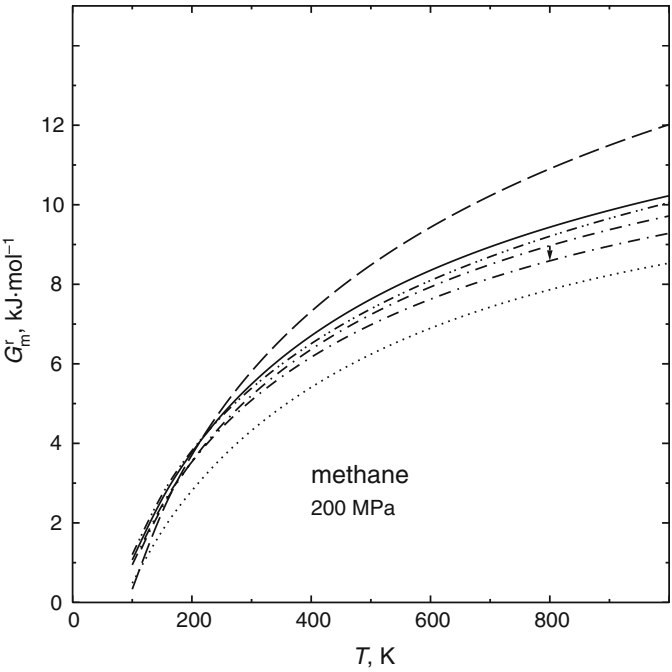

Fig. 13 Prediction of the residual molar Gibbs energy of methane at 200 MPa with several equations of state. — Setzmann and Wagner [5]; for an explanation of the other symbols, see Fig. 11

with

$$a = a_c \alpha(T)$$
$$\xi = \frac{v^*}{V_m}$$
$$\alpha(T) = \left(1 + m(\omega)\left(1 - \sqrt{\frac{T}{T_c}}\right)\right)^2$$

As this equation of state contains a van der Waals repulsion term with fixed covolume, it should not be able to produce an Amagat curve (see Fig. 8). But contrary to expectations, it does. This Amagat curve, however, does not depend on pressure: it is not the consequence of molecular softness, but an artifact caused by the shape of $\alpha(T)$, which has a double zero at $T/T_c = (1 + 1/m)^2$. Consequently, this equation should not be used beyond this temperature (c. 446 K for our parameter set). It is possible, of course, to set $\alpha(T)$ to a constant value beyond some temperature, but this can create problems with some derivatives.

If an adequate accounting for molecular softness is the key to the modeling of dense fluids, it is only logical to test some equations of state for the Lennard-Jones fluid, the system with probably the most comprehensive set of computer simulation data. Fig. 9 shows the characteristic curves of the Lennard-Jones equations of Johnson

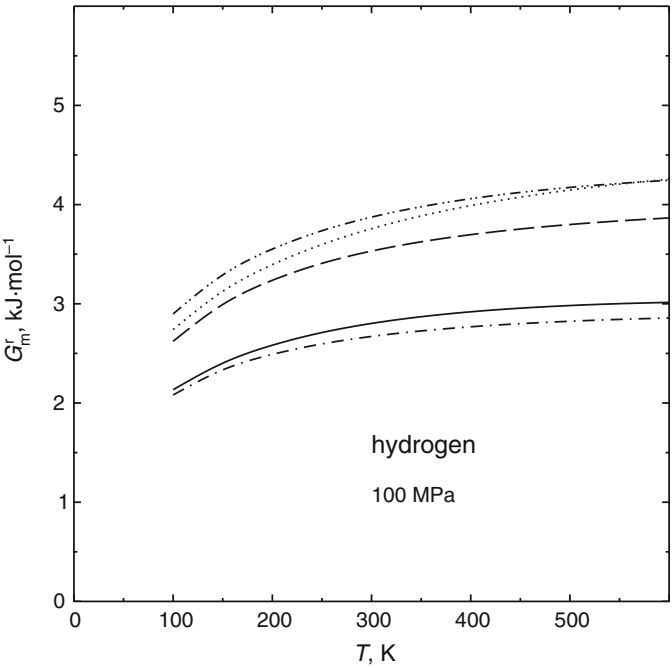

Fig. 14 Prediction of the residual molar Gibbs energy of hydrogen at 100 MPa with several *Lennard-Jones fluid* equations of state. — Leachman et al. [9], –·– sSPHCT (this work), ····· Johnson et al. [23], –··–: Kolafa and Nezbeda [14], – – – Mecke et al. [24]

et al. [23], Kolafa and Nezbeda [14], and Mecke et al. [24]. The equation of Johnson et al. is a modified Benedict–Webb–Rubin equation; the other two equations consist of a hard-sphere term and a 2-dimensional polynomial as the attraction term. The three equations give almost coinciding results for the Boyle and Charles curves, but evidently the equation of Johnson et al. is not as reliable as the other two at extreme pressures and densities. Only the equation of Mecke et al. gives an Amagat curve with the correct shape; for the other two equations, the Amagat curve turns upwards at low temperatures.

3.2 Thermodynamic Functions

An important feature of equations of state is their capability to estimate caloric properties; these would, for instance, be needed to assess the influence of pressure on chemical reactions. Figure 10 shows predictions of the residual molar Gibbs energy of hydrogen at 100 MPa obtained with several SPHCT-based models: original SPHCT, soft-core SPHCT (sSPHCT) with the temperature dependencies of the PC-SAFT equation, and sSPHCT using BH and WCA perturbation theories. It can be seen that the PC-SAFT temperature dependence gives an improvement over the original SPHCT equation, but leads to distortions and a not very good slope. The results from BH and WCA perturbation theory agree well at low temperatures, but at high temperatures

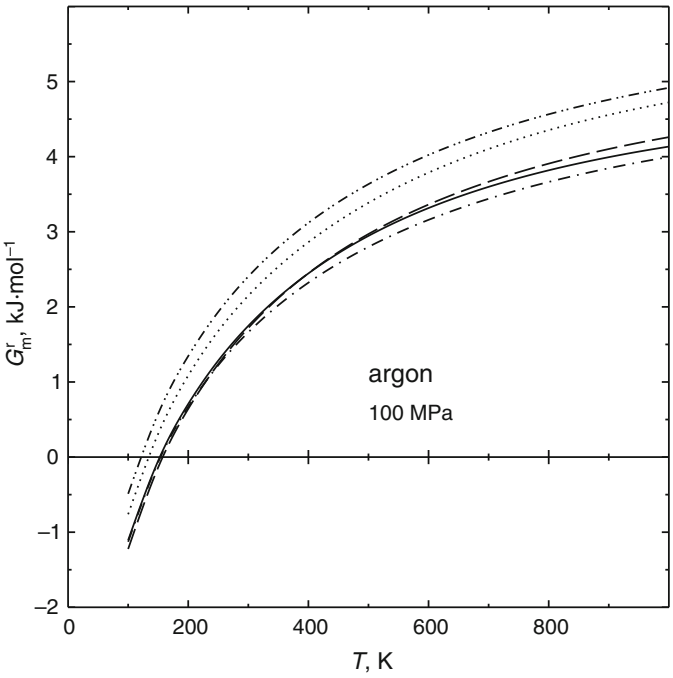

Fig. 15 Prediction of the residual molar Gibbs energy of argon at 100 MPa with several equations of state. — Tegeler et al. [25], –·– sSPHCT (this work), ····· Johnson et al. [23], –··– Kolafa and Nezbeda [14], – – – Mecke et al. [24]

the WCA method with its temperature- and density-dependent collision diameter is clearly better.

Figure 11 shows the same function, but here comparison is made between different equations of state (with their parameters fitted to the critical pressure and temperature). The Peng–Robinson equation gives a surprisingly good prediction under these conditions. The SPHCT equation gives far too high values; inclusion of the softness corrections proposed here improves the predictions very much, and after adding quantum corrections, the agreement with the reference equation of Leachman et al. is reasonably good.

Calculations of the residual molar Gibbs energy for argon at 100 MPa (Fig. 12) and for methane at 200 MPa (Fig. 13) show similar trends. The prediction of the Peng–Robinson equation tends to be somewhat too low that of the SPHCT equation is systematically too high. But after inclusion of the softness correction, this simple equation performs comparable to, and sometimes better than, the sophisticated PC-SAFT equation; furthermore, it behaves better in the vicinity of the Amagat curve.

It is interesting to observe that the three equations for the Lennard-Jones fluid do not match the reference curve for hydrogen very well (Fig. 14). For argon the equation of Mecke et al. is almost on top of the reference curve, whereas the other two equations deviate significantly (Fig. 15).

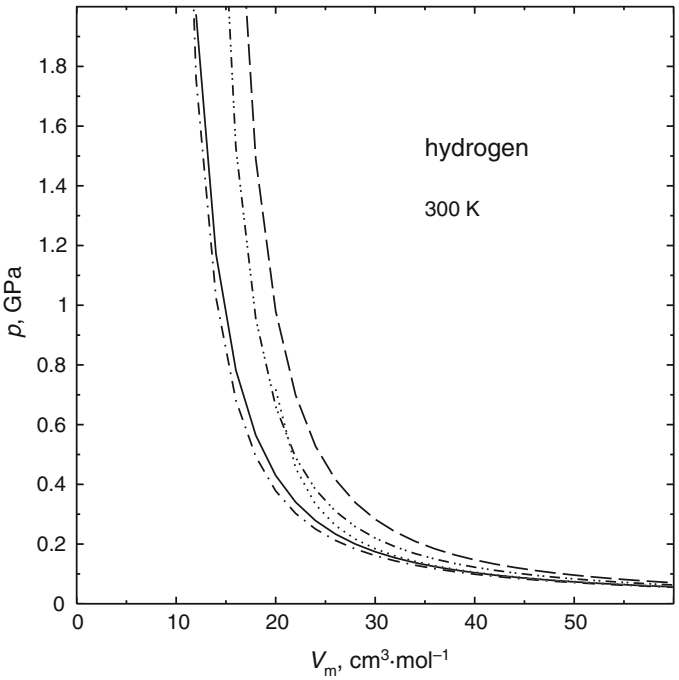

Fig. 16 Pressure of hydrogen as a function of the molar volume at 300 K, calculated with several equations of state. For an explanation of the symbols, see Fig. 11

A comparison of pressure isotherms of hydrogen (Fig. 16) reveals that the sSPHCT prediction follows the empiricial correlation closely beyond 1 GPa, whereas the other equations used here diverge at too large molar volumes. This could possibly be corrected by fitting the size parameters of these equations to the high-pressure part of the isotherm, but then the critical point and the vapor–liquid equilibrium would be shifted.

Residual isochoric heat capacities of fluids are supposed to be positive (with the exception of quantum fluids at low temperatures). On the other hand, one must conclude from Sect. 2.2 that a temperature-dependent molecular size parameter is likely to cause negative $C^{\mathrm{r}}_{V,\mathrm{m}}$ values at high pressures or temperatures for all van der Waals-type equations of state having the structure of Eq. 5. It is therefore interesting to check the predictions of isochoric heat capacities for the equations of state used in this work. Figure 17 shows the boundaries of the negative $C^{\mathrm{r}}_{V,\mathrm{m}}$ regions for hydrogen. These do not correspond to experimental data, but usually indicate a breakdown of the theory or method, and should be avoided in calculations.

- The sSPHCT equation (both with full WCA and BH perturbation theory) can be used down to about $8\,\mathrm{cm}^3 \cdot \mathrm{mol}^{-1}$, with the full method being more stable at high temperatures (for comparison: the critical molar volume is about $73.8\,\mathrm{cm}^3 \cdot \mathrm{mol}^{-1}$).
- The PC-SAFT equation predicts negative $C^{\mathrm{r}}_{V,\mathrm{m}}$ values below about $17\,\mathrm{cm}^3 \cdot \mathrm{mol}^{-1}$
- The empirical equation of Leachman et al. has a small region of negative $C^{\mathrm{r}}_{V,\mathrm{m}}$ below 200 K, i.e., for cold, compressed hydrogen. This region is probably not an

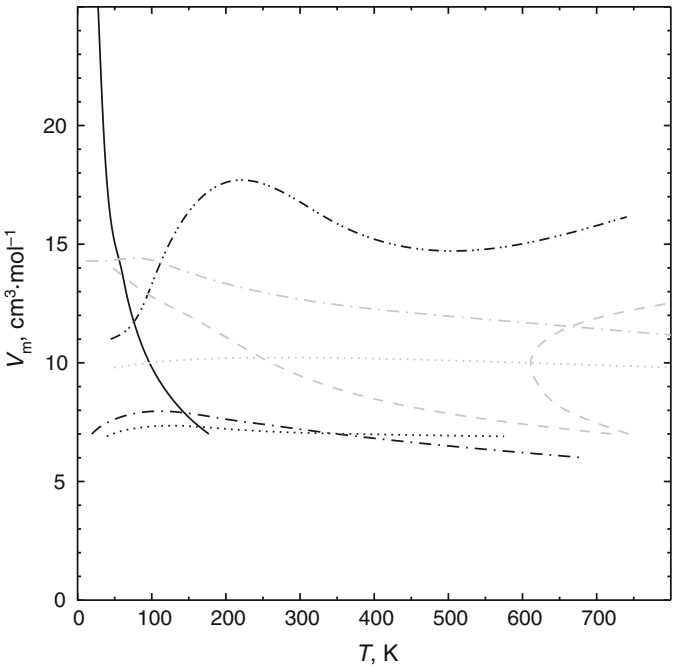

Fig. 17 Boundary below which the residual isochoric heat capacity of hydrogen turns negative. — empirical equation of state of Leachman et al. [9], –·– sSPHCT (this work), WCA perturbation theory, ····· sSPHCT, BH perturbation theory, –··– PC-SAFT; *gray curves* equations of state for the Lennard-Jones fluid, ····· Johnson et al. [23], –··– Kolafa and Nezbeda [14], – – – Mecke et al. [24]. The SPHCT and PR equations do not have regions of negative $C^{\mathrm{r}}_{V,\mathrm{m}}$ in the indicated temperature range

artifact, but real, and the result of quantum effects (see Eq. 26). The pressure along the curve varies from 200 MPa at 25 K to 10 GPa at 200 K.

- The three equations of state for the Lennard-Jones fluid can be used above 10 cm^3 · mol^{-1} (Johnson et al. [23]) or 15 cm^3 · mol^{-1} (Kolafa and Nezbeda [14], Mecke et al. [24]). The equation of Mecke et al. has an additional boundary where its pressures turn negative.
- The SPHCT and PR equations do not give negative $C^{\mathrm{r}}_{V,\mathrm{m}}$ values in the temperature range of Fig. 17, but are of course very inaccurate at high pressures and temperatures.

It thus turns out that, of the theoretical equations of state suited for high-pressure studies, the sSPHCT equation has the largest stable density range.

Figure 18 shows predictions of the residual isobaric heat capacity of hydrogen at 100 MPa for several equations of state. Again it turns out that the sSPHCT method gives reasonably good results, whereas the PC-SAFT equation predicts a region of negative residual heat capacities[3] and a wrong slope.

[3] As discussed above, residual *isobaric* heat capacities can have negative values. In our example, however, the experimental data are positive.

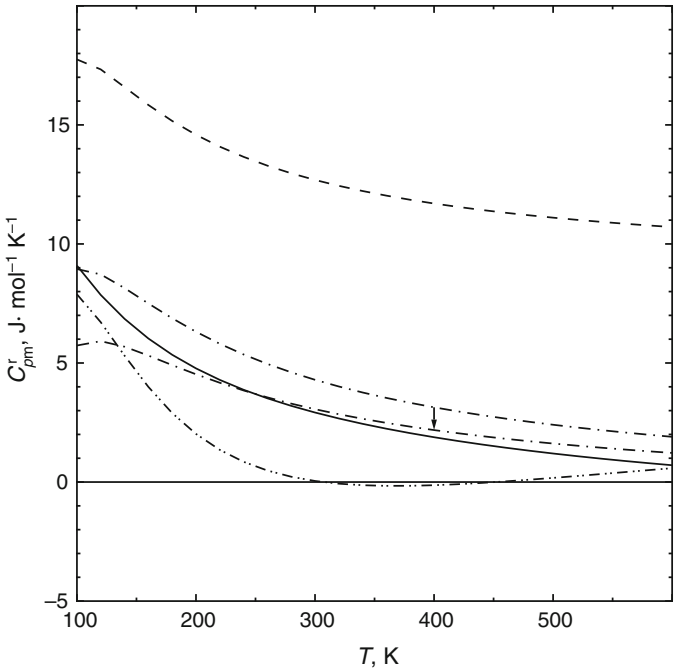

Fig. 18 Residual isobaric heat capacity of hydrogen at 100 MPa; for an explanation of the symbols, see Fig. 11

4 Conclusion

Soft repulsion can be represented by means of a temperature- and density-dependent collision diameter, which can be obtained from WCA perturbation theory. This implies an iterative procedure, but there are efficient iteration schemes that keep the numerical effort tolerable.

Equations of state containing a hard-core equation as a repulsion term usually do not yield Amagat curves, one of Brown's characteristic curves for the assessment of the quality of equations of state. Introduction of the softness correction proposed here leads to physically reasonable Amagat curves.

The temperature dependence of the softness correction is rather critical. A common semiempirical function based on a Boltzmann factor is shown to cause distorted Amagat curves and inferior predictions of thermodynamic functions at high pressures.

It seems that a carefully constructed, theory-based repulsion term in an equation of state is of central importance if the equation is to cover a wide range of densities and temperatures. Deficiencies of the repulsion term cannot be compensated by sophisticated repulsion terms.

We conclude that the application range of equations of state can be significantly extended by properly accounting for soft repulsion, and that even simple equations of state with a good theoretical background (like the SPHCT equation used in this work) can be reliable tools for high-pressure studies.

Acknowledgments The authors wish to thank Sergio E. Quiñones-Cisneros (National Autonomous University of Mexico, Mexico City) for drawing their attention to the problem, and J. Leachman (University of Idaho, Moscow) and E. W. Lemmon (NIST, Boulder) for making their hydrogen equation of state available as well as for helpful discussions. Olga Boshkova was supported by a scholarship of the German Academic Exchange Service (DAAD). Financial support by the Fonds of the German Chemical Industry is gratefully acknowleged.

A1. Steffensen's Accelerated Substitution Method

For the successive substitution method the equation to be solved is cast in the form

$$x = f(x), \tag{30}$$

where $f(x)$ is the so-called step function. Substitution of an approximation for the solution, x_0, into the equation yields an improved approximation, $x_1 = f(x_0)$, which in turn can be substituted into the equation. The method converges only if $\left|\frac{\mathrm{d}f(x)}{\mathrm{d}x}\right| < 1$, and then usually with merely linear convergence order.

Steffensen's method consists of a linear extrapolation of two successive substitution steps:

$$\begin{aligned} x_1 &= f(x_0) \\ x_2 &= f(x_1) \\ x_{2,\mathrm{S}} &= x_0 - \frac{(x_1 - x_0)^2}{x_2 - 2x_1 + x_0} \end{aligned} \tag{31}$$

$x_{2,\mathrm{S}}$ is then used for the next iteration cycle. As long as the denominator in the extrapolation formula is different from zero, the $x_{i,\mathrm{S}}$ converge—even when the slope criterion is not fulfilled—with quadratic convergence order.

References

1. E.H. Brown, Bull. Int. Inst. Refrig. Paris, Annexe **1960–1961**, 169 (1960)
2. U.K. Deiters, K.M. de Reuck, Pure Appl. Chem **69**, 1237 (1997)
3. E. Bender, *The Calculation of Phase Equilibria from a Thermal Equation of State Applied to the Pure Fluids Argon, Nitrogen, Oxygen and their Mixtures* (Verlag C. F. Müller, Karlsruhe, 1973)
4. R.T. Jacobsen, R.B. Stewart, J. Phys. Chem. Ref. Data **2**, 757 (1973)
5. U. Setzmann, W. Wagner, J. Phys. Chem. Ref. Data **20**, 1061 (1991)
6. O. Kunz, R. Klimeck, W. Wagner, M. Jaeschke, *The GERG-2004 Wide-Range Reference Equation of State for Natural Gases*. GERG (European Gas Research Group) Technical Monographs, vol. 15. (VDI-Verlag, Düsseldorf, 2007)
7. M.A. Trebble, P.R. Bishnoi, Fluid Phase Equilib. **29**, 465 (1986)
8. P.H. Salim, M.A. Trebble, Fluid Phase Equilib. **65**, 59 (1991)
9. J.W. Leachman, R.T. Jacobsen, S.G. Penoncello, E.W. Lemmon, J. Phys. Chem. Ref. Data **38**, 721 (2009)
10. H.C. Andersen, J.D. Weeks, D. Chandler, Phys. Rev. A **4**, 1597 (1971)
11. L. Verlet, J.J. Weis, Phys. Rev. A **5**, 939 (1972)
12. K. Lucas, *Angewandte Statistische Thermodynamik* (Springer, Berlin, 1986)
13. G. Jordan-Engeln, F. Reutter, *Numerische Mathematik für Ingenieure* (Bibliographisches Institut, Mannheim, 1985)

14. J. Kolafa, I. Nezbeda, Fluid Phase Equilib. **100**, 1 (1994)
15. C.-H. Kim, P. Vimalchand, M.D. Donohue, S.I. Sandler, AIChE J. **32**, 1726 (1986)
16. U.K. Deiters, Chem. Eng. Technol. **23**, 581 (2000)
17. U.K. Deiters, *ThermoC* project homepage http://thermoc.uni-koeln.de/index.html
18. Y. Singh, S.K. Sinha, Phys. Rep. **79**, 213 (1981)
19. J. Gross, G. Sadowski, Fluid Phase Equilib. **168**, 183 (2000)
20. J. Gross, G. Sadowski, Ind. Eng. Chem. Res. **40**, 1244 (2001)
21. D.Y. Peng, D.B. Robinson, Ind. Eng. Chem. Fundam. **15**, 59 (1976)
22. G. Soave, Chem. Eng. Sci. **27**, 1197 (1972)
23. J.K. Johnson, J.A. Zollweg, K.E. Gubbins, Mol. Phys. **78**, 591 (1993)
24. M. Mecke, A. Müller, J. Winkelmann, J. Vrabec, J. Fischer, R. Span, W. Wagner, Int. J. Thermophys. **17**, 391 (1996)
25. C. Tegeler, R. Span, W. Wagner, J. Phys. Chem. Ref. Data **28**, 779 (1999)